Reconfigurable optical spectra from perturbations on elliptical whispering gallery resonances

Makan Mohageg[1] **and Lute Maleki**

Jet Propulsion Laboratory, California Institute of Technology, 4800 Oak Grove Drive, Pasadena, California 91109-8099

[1] *Current address: Department of Applied Physics, California Institute of Technology, Pasadena, CA 91125, USA.*

makan@caltech.edu

Abstract: Elastic strain, electrical bias, and localized geometric deformations were applied to elliptical whispering-gallery-mode resonators fabricated with lithium niobate. The resultant perturbation of the mode spectrum is highly dependant on the modal indices, resulting in a discretely reconfigurable optical spectrum. Breaking of the spatial degeneracy of the whispering-gallery modes due to perturbation is also observed.

OCIS codes: (230.5750) Resonators; (120.2440) Filters; (130.3730) Lithium niobate

References and links

1. A. Ashkin and J. M. Dziedzic, "Observation of optical resonances of dielectric spheres by light scattering," Appl. Opt. **20**, 1803 (1981)
2. V. B. Braginsky, M. L. Gorodetsky and V. S. Ilchenko, "Quality-factor and nonlinear properties of optical whispering gallery mode," Phys. Lett. A, **137**, 393397 (1989).
3. S. C. Hill and R. E. Benner,"Morphology-dependent resonances," in *Optical Effects Associated with Small Particles* , P. W. Barber and R. K. Chang, eds., (World Scientific, 1988) pp. 7-34.
4. V. S. Ilchenko, A. A. Savchenkov, A. B. Matsko and L. Maleki, "Dispersion compensation in whispering-gallery modes," J. Opt. Soc. Am. A **20**, 157 (2003).
5. M. L. Gorodetsky, A. A. Savchenkov and V. S. Ilchenko, Opt. Lett., "Ultimate Q of optical microsphere resonators," **21**, 453 (1996).
6. A. A. Savchenkov, V. S. Ilchenko, A. B. Matsko and L. Maleki, Phys. "Kilohertz optical resonances in dielectric crystal cavities," Rev. A, **70**, 051804(R) (2004).
7. D. W. Vernooy, A. Furusawa, N. Ph. Georgiades, V. S. Ilchenko and H. J. Kimble, Phys. Rev. A, "Cavity QED with high-Q whispering gallery modes," **57**, R2293 (1998).
8. S. M. Spillane, T. J. Kippenberg, K. J. Vahala, K. W. Goh, E. Wilcut, and H. J. Kimble "Ultrahigh-Q toroidal microresonators for cavity quantum electrodynamics," Phys. Rev. A, **71**, 013817 (2005).
9. A. A. Savchenkov, V. S. Ilchenko, A. B. Matsko and L. Maleki, "Tunable Filter Based on Whispering Gallery Modes," Electron. Lett., **39**, No. 4, 389 (2003).
10. T. Indukuri, P. Koonath and B. Jalali, "Three-dimensional integration of metal-oxide-semiconductor transistor with subterranean photonics in silicon," App. Phys. Lett., **88**, 121108 (2006).
11. J. E. Ford and J. A.Walker "Dynamic Spectral Power Equalization Using Micro-Opto-Mechanics," IEEE Photon. Technol. Lett., **10**, 1440 (1998).
12. J. E. Ford, V. A. Aksyuk, D. J. Bishop and J. A. Walker "Wavelength Add-Drop Switching Using Tilting Micromirrors," J. Lightw. Technol., **17**, 904 (1999).
13. T. Sano, T. Iwashima, M. Katayama, T. Kanie; M. Harumoto, M. Shigehara, H. Suganuma and M. Nishimura "Novel multichannel tunable chromatic dispersion compensator based on MEMS and diffraction grating," IEEE Photon. Technol. Lett., **15**, 1109 (2003).
14. N. Ph. Georgiades, E. S. Polzik and H. J. Kimble, "Atoms as nonlinear mixers for detection of quantum correlations at ultrahigh frequencies," Phys. Rev. A, **55**, R1605 (1997).

#89275 - $15.00 USD Received 1 Nov 2007; revised 4 Jan 2008; accepted 4 Jan 2008; published 29 Jan 2008

15. M. Porrati and S. Putterman, "Wave-function collapse due to null measurements: The origin of intermittent atomic fluorescence ," Phys. Rev. A, **36**, 929 (1987).
16. A. Dantan, A. Bramati and M. Pinard, " Atomic quantum memory: Cavity versus single-pass schemes," Phys. Rev. A, **71**, 043801 (2005).
17. M. Mohageg, A.A. Savchenkov, and L. Maleki, "High-Q optical whispering gallery modes in elliptical LiNbO3 resonant cavities," Opt. Express, **15**, No. 8, 4869 (2007).
18. V.S. Ilchenko, P.S. Volikov, V.L. Velichansky, F. Treussart, V. Lefevre-Seguin, J.-M. Raimond and S. Haroche, "Strain-tunable high-Q optical microsphere resonator," Opt. Comm., **145**, No. 1, 86 (1988).
19. V. S. Ilchenko, A. A. Savchenkov, A. B. Matsko and L. Maleki, "Nonlinear Optics and Crystalline Whispering Gallery Mode Cavities," Phys. Rev. Lett., **92**, 043903 (2004).
20. Makan Mohageg, D. V. Strekalov, A. A. Savchenkov, A. B. Matsko, V. S. Ilchenko, and L. Maleki, "Calligraphic poling of Lithium Niobate," Opt. Express, **13**, No. 9, 3408 (2005).
21. M. Mohageg, A. A. Savchenkov, D. Strekalov, A. B. Matsko, V.S. Ilchenko and L. Maleki, "Reconfigurable optical filter," Electron. Lett. **41**, No. 6 (2005).
22. A. B. Matsko, L. Maleki, A. A. Savchenkov, and V. S. Ilchenko, "Whispering gallery mode based optoelectronic microwave oscillator," J. Mod. Opt. **50**, No. 15, 2523-2542 (2003).
23. H. Rokhsari, T. J. Kippenberg, T. Carmon, and K. J. Vahala, "Radiation-pressure-driven micro-mechanical oscillator," Opt. Express, **13**, No. 14, 5000 (2005).

1. Introduction

Since the first demonstration of high-Q optical whispering gallery mode (WGM) resonators with liquid droplets [1] and glass microspheres [2], these devices have found numerous applications in various fields of science and technology. Optical WGM resonators have high quality factors and associated narrow resonances, and an observation of optical modes with kilohertz WGM linewidths has recently been made [6] in resonators made from CaF_2[5]. Because of the readily achievable high Q-factors, WGM resonators are attractive and practical for applications in cavity quantum electrodynamics studies [7, 8]. Additionally, high-Q WGM resonances have been used as narrowband optical filters for data transmission [9], and as novel optical multiplexers [10]. These demonstrations have all been made with resonators having fixed spectra. The mode frequencies of the WGMs are determined by the resonator radius and the refractive index of the host material [3, 4]. In spherically symmetric boundaries, the spectrum is highly degenerate, but any modification of the resonator morphology can break this degeneracy. For instance, a spherical resonator could be converted to a thin disk-shaped resonator by removing the polar regions. This breaks the degeneracy of the angular modes.

But engineering the spectrum of a WGM resonator can significantly extend the range of its applications, and provide functionalities that are difficult or impossible to achieve otherwise. An example of such an application is the optical domain microwave filter made with lithium niobate with tunability across more than an octave of frequency [9]. Nevertheless, a tunable modal spectrum is not the optimal solution for many applications. Ideally, the spectrum should also be reconfigurable. By reconfigurable we mean that the resonant frequencies of the individual modes should move at different rates under the same forcing influence. With reconfigurable spectra, WGM resonators could find many additional applications. A single reconfigurable WGM resonator, for example, could also be used as a multipole passband filter to achieve variable optical attenuation [11], add-drop multiplexing [12], and dispersion compensation [13]. In this letter we report on the demonstration of discrete tuning of the mode frequencies of high-Q, elliptical whispering-gallery-mode (WGM) resonators made from $LiNbO_3$.

The narrowband, reconfigurable spectra reported in this article could be useful in a number of other applications related to quantum optics and photonic communications. From the perspective of cavity quantum electrodynamics, a reconfigurable spectrum will enable evanescent coupling of two resonant modes to two atomic transitions, to allow, for example, measurement of the correlation between those transitions [14]. Indeed, measurement of any quantum process that involves more than one atomic transition (such as quantum non-demolition measurement

#89275 - $15.00 USD Received 1 Nov 2007; revised 4 Jan 2008; accepted 4 Jan 2008; published 29 Jan 2008

[15] and electronically induced transparency [16]) will be facilitated by utilization of an appropriately reconfigured, narrowband optical resonance spectrum such as the one described in this article.

The paper begins with an introduction to the tuning of WGM spectra, followed by a description of the experiments conducted with elliptical resonators. WGMs with Q-factor in excess of 10^7 input coupled at efficiencies greater than 97% in resonators with elliptical cross section made from $LiNbO_3$ were first reported in Ref. [17]. We hypothesize that the application of a local perturbation along the boundary these highly asymmetric structures would result in a reconfigurable spectrum. To confirm this, we measured the response of the transmission spectra under the application of uniform electrical bias (dc, ac, and rf,) the application of anisotropic stress along the resonator axis, and the application of a local deformation at two regions along the equator (perpendicular to the axis) of the elliptical resonator.

2. Tuning WGM Resonances

Tuning the resonant frequencies of dielectric microsphere WGMs was first demonstrated through the application of elastic strain along the polar axis of the sphere [18]. In this case the observed shift in resonance frequency obeys the equation

$$\frac{\Delta\nu}{\nu} = -\frac{\Delta r}{r} - \frac{\Delta n}{n} + \frac{(\ell - m)}{\ell}(\Delta e)^2 \tag{1}$$

The first term is the fractional change in resonator radius due to squeezing, the second term is the fractional change in refractive index due to the photo-elastic effect, and the last is a term proportional to the changing eccentricity of the initially spherical resonator. The last term is also proportional to the difference between polar and azimuthal modal indices, and thus should in principle produce variable tuning rates. However, strain induced change in eccentricity is vanishingly small when compared to photo-elastic shifts in the refractive index and the strain induced change in effective radius. Furthermore, in large resonators, the azimuthal quantum number ℓ is large. The inherent discreetness in the tuning rate is compromised by the spherical symmetry of the resonator structure.

Advances in fabrication techniques has led to the development of disk shaped WGM resonators constructed from lithium niobate [19]. Electro-optic tuning of the resonator spectra has been demonstrated [9]. Application of an electric field across the lithium niobate resonators causes the resonant frequencies of all modes to shift uniformly at the same rate by the Pockell's effect.

$$\frac{\Delta\nu}{\nu} = \frac{\Delta n}{n} = -\frac{1}{2}n^2 r_{ij} \cdot \frac{V}{T} \tag{2}$$

A bias voltage V applied across material with thickness T in the direction characterized by indices *ij* experiences a fractional change in modal frequency ν (or refractive index n) proportional to the zero voltage index and the appropriate linear electro optic coefficient r_{ij}. For materials that do not posses inversion symmetry, application of voltage can shift refractive index by interaction with the third order optical susceptibility via the Kerr effect.

A WGM based, electro-optical reconfigurable filter was also demonstrated by using lithium niobate resonators with a ferroelectric poling structure [20] resembling numerous concentric rings [21]. The thicknesses of the ring-shaped domains were determined by the predicted radial field distributions of the WGMs. Mode fields overlap with ferroelectric regions that are either parallel or antiparallel with the resonator axis. When a DC bias is applied, the mode frequencies shift as predicted in Eq. 2, however the sign of the frequency shifts depend on the orientation of the local ferroelectric domain. The net result on a WGM depends on the overlap of the

#89275 - $15.00 USD Received 1 Nov 2007; revised 4 Jan 2008; accepted 4 Jan 2008; published 29 Jan 2008

mode field with the ferroelectric structure. Specifically, modes with different radial indices have different overlaps with the poling structure. A voltage applied across the z-axis of the resonator shifts the resonant frequency in proportion to this overlap. The resultant tuning rate depends on modal indices. It can be positive, negative, or nearly zero. The reconfigurability depends on the structure of ferroelectric domains, which is in turn determined by the wavelength of light to be used.

Here we report on the demonstration of tuning and reconfigurable spectra of high-Q WGMs in elliptical resonators. Application of a DC field causes all the modes to shift at the same rate. Application of elastic strain across the resonator axis results in tuning rates that are different for modes closer to or further from the source of the strain. Mechanical tuning of asymmetric resonators results in highly discreet tuning rates that are related to the modal indices. This is, in effect, a reconfigurable optical spectra that will be immune to electromagnetic interference. Additionally, mechanical tuning results in symmetry breaking of the modal spatial profiles.

3. Experiment

A WGM resonator with elliptical cross-section was fabricated from congruent $LiNbO_3$ using mechanical grinding and polishing. The thickness of the resonator was 500 μm. The semiminor axis length was 3.5 mm, the semimajor axis length is 4.4 mm, which gives an eccentricity of .71. Laser light of 1.55 μm wavelength was evanescently coupled to the resonator through a diamond prism. The frequency of the laser light was scanned over 25 GHz at a rate of 20Hz. The free spectral range of the resonator was about 11 GHz, so the laser scan covered more than two free spectral ranges (FSRs.) The Q-factor of the modes was greater than 10^7. Light exiting the resonator through the diamond prism was collected by a 3 mm diameter light pipe and sent to a photodiode. The resonator was mounted on top of a metal substrate. A picture of a coupled elliptical resonator and a schematic of the tuning scheme is provided in (Fig. **??**).

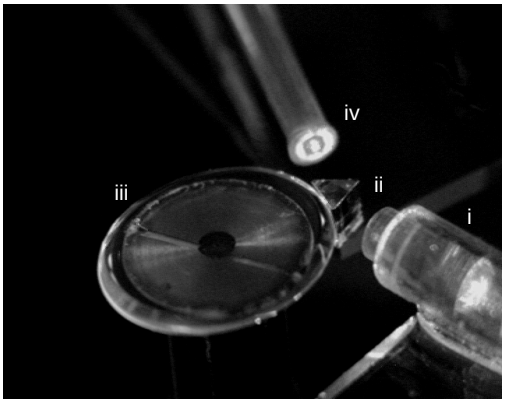

Fig. 1. Picture of a coupled WGM resonator with elliptical cross-section. A fiber pigtailed GRIN lens (i) launches the light beam with appropriate numeric aperture and incident angle into the diamond prism (ii.) The resonator (iii) is separated from the prism surface by some fraction of a μm to ensure critical coupling. Light exiting the resonator through the prism is collected in the light pipe (iv) and sent to a photodiode (not shown.) Other exit channels exist of the light in the WGM, particularly scattering from surface defects and internal defects. These exit channels contribute to loss and are characterized by broader linewidths and reduced overall coupling.

#89275 - $15.00 USD Received 1 Nov 2007; revised 4 Jan 2008; accepted 4 Jan 2008; published 29 Jan 2008

Three types of perturbation were applied to an elliptical resonator to tune the frequency of the WGMs.: 1) Electrical bias was applied across the resonator axis to produce a uniform shift in refractive index that affects all modes uniformly; 2) Elastic strain was applied across the resonator axis to produce a shift in mode frequencies that is dependant on the radial index of the modes; and 3) a localized deformation along the equator of the resonator to produce a shift in mode frequencies that is dependant on all modal indices.

Only modes that demonstrated a coupling efficiency of greater than 20% were used. In some of the cases described below, certain modes were observed to shift at the same rate. A group of modes that shift at the same rate is henceforth referred to as a mode family.

3.1. Electrical Bias

The first experiment used a uniform electric field to shift the frequencies of all spectral resonances. Dc electric bias was applied across the top and bottom surface of the resonator to shift the index of refraction in linear proportion to the bias voltage.

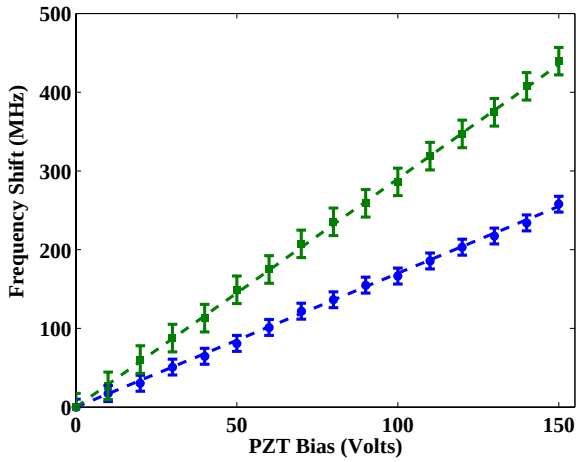

Fig. 2. Schematic of the active frequency lock used to lock the laser frequency to the cavity resonance. S_{12} is the resonator reflection spectra.

Colloidal graphite was applied in a uniform layer to the top and bottom surface of the resonator to create low frequency electrodes. The edge of the graphite layer was 50 μm away from the resonator edge, where the bulk of the optical field is present. The effective overlap between the mean optical field and the dc bias field was thus calculated to be 16%.

When the voltage bias was applied, the frequency of each resonance shifted at a rate of 5.2 $\pm$ .1 MHz/V. This tuning rate is close to the value predicted by Pockell's effect, 5.11 MHz/V for a 16% overlap. All modes were observed to shift at the same rate.

The same experimental setup was used to explore ac switching rates of the mode frequencies. Ac bias was applied at 1 kHz, 10 kHz, 100 kHz, and 1 MHz. The time constant of the switch was measured for all modes. Across all frequencies and all resonant modes, a switching rate of 35 $\pm$ 1 ns was measured. The fast switching speed observed is primarily due to the large thickness of the resonator. If the resonator thickness was 100 μm instead of 500 μm, the switching rate would have been 25 times slower.

The final set of experiments conducted with electrical bias involved a demonstration of rf modulation of the elliptical WGMs. The general ideas and experimental approach implemented were adapted from Ref. [22]. To increase the overall efficiency of the rf-optical interaction, a

#89275 - $15.00 USD Received 1 Nov 2007; revised 4 Jan 2008; accepted 4 Jan 2008; published 29 Jan 2008

second elliptical resonator was constructed with thickness 100 μm. The eccentricity of this resonator was .65, with a FSR of 4.8 GHz. A 'horseshoe' shaped metal electrode was placed into direct contact with the top surface of the resonator. The bottom of the resonator was in direct contact with an extended electrode. The horseshoe electrode was galvanicly coupled to a 50 Ω microwave strip waveguide. The frequency of the laser was locked to a resonator mode using a Pound-Drever-Hall locking scheme (Fig. **??**). Once the lock is stable, an rf signal at twice the FSR is sent through the waveguide and into the resonator. Optical sidebands were produced at twice FSR (Fig. **??**).

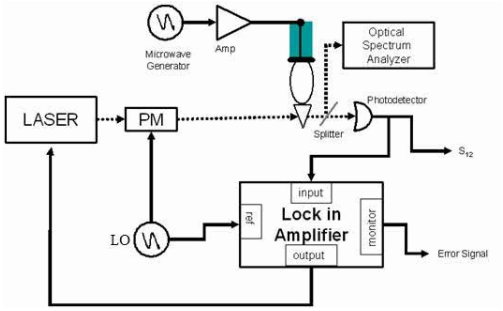

Fig. 3. Spectrum demonstrating interaction of optical mode with rf field. The rf frequency was set to twice the optical FSR. The efficiency of rf-optical interactions is predicted to be large when the rf frequency corresponds to the spacing between two optical modes.

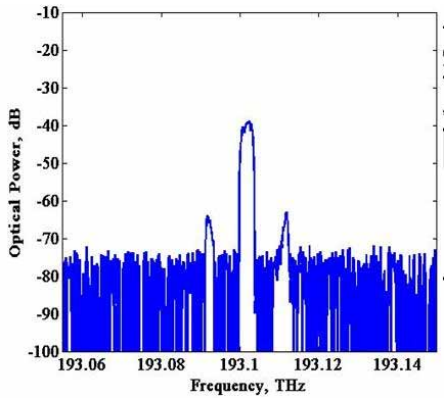

Fig. 4. Shift in mode frequencies as a function of PZT voltage. Two discreet tuning rates are apparent, corresponding to mode families (green squares and blue circles) with different radial modal indices.

The coupling efficiency of microwaves sent into the horseshoe was measured by monitor-

#89275 - $15.00 USD Received 1 Nov 2007; revised 4 Jan 2008; accepted 4 Jan 2008; published 29 Jan 2008

ing the back reflected microwave power on a network analyzer. The coupling efficiency was 25%. Microwave power was gradually increased until optical sidebands were evident on the optical spectrum analyzer. The sidebands became visible at microwave power of 15 dB. Incidentally, this amount of microwave power was only slightly smaller than the amount required to heat the resonator and cause temperature shifts of the mode frequency. The efficiency of the microwave-optical interaction presented in this article is low, but can likely be increased with additional effort. To our knowledge, this is the first demonstration of any nonlinear process in an asymmetric optical WGM resonator.

3.2. Elastic Strain

The results of dc and ac modulation show that perturbations that are effectively global result in uniform shifts in all resonance frequencies. The next experiment uses strain along the z-axis to apply a perturbation that exhibits a strong spatial dependence. The spatial dependence of this perturbation results in frequency shifts that are different for modes with different radial index.

Elastic strain was applied to the loaded resonator by squeezing the structure along its axis using a PZT. The PZT was placed on the top surface of the resonator. The top of the PZT was in contact with a stainless steel plate that connected to a c-clamp. The bottom end of the c-clamp was the surface upon which the resonator was mounted. A glass plate between the PZT and the top plane of the resonator distributed the strain isotropically across the resonator. The spectrum of the resonator was recorded as a function of voltage applied to the PZT. As the PZT voltage was increased, the resonance frequencies of the resonator shifted linearly (Fig. **??**).

The incident angle of the laser beam was 25^o. Several modes were coupled to with varying efficiency. As the PZT voltage was increased, the resonator mode frequencies shifted at different rates. Two modes tuned at a rate of 2.9 MHz/V, while the other 11 modes tuned at a rate of 1.7 MHz/V. The incident angle of the laser beam was reduced to 22^o (which is the critical angle for diamond-$LiNbO_3$ TM-WGM interface.) The coupling efficiency to the two faster modes decreased to nearly zero, and the observed shift in frequencies of all efficiently coupled modes was found to be 1.7 MHz/V.

The surface area of the glass plate used to distribute the strain generated by the expansion of the PZT was smaller than the surface area of the elliptical resonator. Thus the strain on the resonator was not uniform, but concentrated towards the center. Modes that have higher radial index have a larger overlap with the regions of greater strain, and thus tune at a faster rate than modes with lower radial index. Two distinct tuning rates were observed initially. When the geometry of the coupling scheme was varied to guarantee coupling into modes of only one radial index only a single tuning rate was observed. We conclude that application of inhomogeneous strain along the z-axis of the resonator causes resonant frequency shifts that are related to the radial modal index of the resonances.

3.3. Localized Perturbation

Our starting point in this investigation is the hypothesis that local perturbations applied to an asymmetric resonator will cause discrete frequency tuning in the resonator spectrum. After investigating the effects of uniform perturbation (applied voltage) and radially anisotropic perturbation (stress) we are now prepared to explore the effects caused by a localized deformation. To test our hypothesis, strain was applied to the elliptical resonator along the semimajor and semiminor axes of the ellipse. The effect of the strain is a circular deformation in resonator geometry that overlaps with modes in proportion to the difference between azimuthal and polar indices.

To apply and quantify the strain, a glass plate perpendicular to the resonator plane was placed opposite the coupling prism. The glass plate was placed into contact with the resonator. As long

#89275 - $15.00 USD Received 1 Nov 2007; revised 4 Jan 2008; accepted 4 Jan 2008; published 29 Jan 2008

as the glass plate is clean and devoid of surface defects, placing it at or near the resonator surface will not cause additional loss. This is because the refractive index of the plate is less than that of the resonator, thus the light confined within the resonator by total internal reflection cannot exit through the glass. A voltage applied to a PZT connected to the glass plate caused the glass plate to deform the resonator. A schematic of the process is shown in (Fig. **??**.) Interference of white light at the glass plate/resonator surface interface was used to quantify the size of the deformation (Fig. **??**.) For purposes of comparison, the experiment described here was performed on the elliptical resonator as well as a resonator with circular cross section.

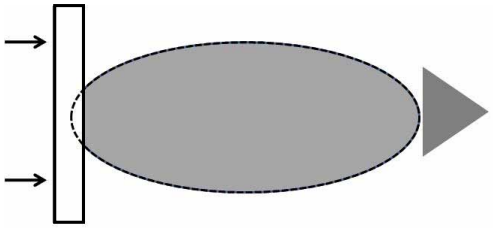

Fig. 5. Top-down schematic of the method used to produce a geometric deformation along the resonator equator. A glass plate was pressed against the resonator equator at the position opposite the diamond prism.

In a perfectly spherical resonator, or a disk-shaped resonator with circular cross section, the overlap of the various (ℓ-m) modes with a circular deformation follows odd-even symmetry. This is because the way the angular component of the mode eigenfunction (a spherical harmonic) overlaps with any deformation along the equator. Spherical harmonics with even (ℓ - m) index have zero overlap, while spherical harmonics with odd or zero index have a nonzero overlap. Physically, this predicts that if a spherical or disk shaped WGM resonator is squeezed along the equatorial plane, the frequencies of the even modes will not shift, while the frequencies of the odd modes will shift in proportion to their particular (ℓ - m) index. To test this prediction, we carried out the experiment. The results are shown in (Fig. **??**.) The size of deformation corresponds to the radius of the deformation, which is measured directly through interferometric techniques. This value is proportional to the square root of the PZT voltage.

Not all of the modes that shift in frequency do so at the same rate. This is because the modes may have different radial index. Modes that are closer to the edge are expected to shift at a faster rate than modes further from the edge. There should also be a residual frequency shift in all modes due to the photo-elastic strain in the region about the deformation, although this was not observed in our measurements. This could be due to the inherently slow tuning rates observed; perhaps with larger diameters of perturbation the background photo-elastic shift becomes more prominent.

The same experiment was carried out on the WGM resonator with elliptical cross-section. In this case, different frequency shifts were observed for the same modes depending on the location of the deformation. Specifically, squeezing the resonator along the semiminor axis

#89275 - $15.00 USD Received 1 Nov 2007; revised 4 Jan 2008; accepted 4 Jan 2008; published 29 Jan 2008

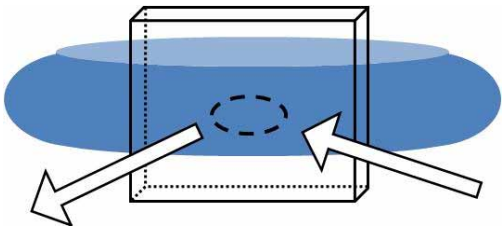

Fig. 6. Side-view schematic of the deformation. The two arrows represent white light that is incident at the interface between the glass plate and the resonator surface. The reflected interference pattern is imaged and used to calculate the size of the deformation, characterized in units of nanometers in the y-axis of (Fig. **??**). The gap between the prism and the resonator edge was maintained to ensure critical coupling throughout the application of strain.

yields different frequency shifts than squeezing it along the semimajor axis. The measured rates of tuning (the slopes of the curves in Fig. **??**) were measured and are presented in (Table 1.) Odd-even symmetry is not immediately apparent in the response of the elliptical resonators to the perturbation; discrete tuning rates of tuning were none the less observed (Table 1.)

Table 1. Discrete tuning rates of the modes

Mode Number	1	2	3	4	5	6	7
Semimajor Axis	11·a	0	5·a	2·a	5·a	2·a	28·a
Semiminor Axis	+5/2·b	-5/2·b	±0	±0	-5/2·b	-b	+b
Mode Number	8	9	10	11	12	13	1*
Semimajor Axis	a	3·a	a	a	3·a	11·a	11·a
Semiminor Axis	-5/2·b	+b	±0	±0	-5/2·b	+b	+5/2·b

In (Table 1), modes are assigned number based on their frequency. Mode "1" corresponds to the first mode in a given free spectral range that is coupled at greater than 20% efficiency. Mode "2" is the next mode, with slightly higher frequency, in the same FSR, and so forth. There were 13 unique modes that were coupled to with greater than 20% efficiency. Mode "1*" corresponds in frequency to the frequency of mode "1" plus 11 GHz: the resonator FSR. Tuning rates were collected for the 13 modes over two FSRs. In addition, the center frequency of the laser was shifter thermally by .5 nm and the experiment was repeated for another two FSRs worth of modes. Modes with the same mode number in the various FSR shifted at the rates shown in (Table 1) with variation smaller than 5 kHz/nm.

When the perturbation (stress) is applied along the semimajor axis, one mode per FSR did not shift at all through the range of perturbation- the frequency of this mode is stationary while the frequency of all other modes is changed. Successive modes shift at integer multiples of a = 706 kHz/nm.

#89275 - $15.00 USD Received 1 Nov 2007; revised 4 Jan 2008; accepted 4 Jan 2008; published 29 Jan 2008

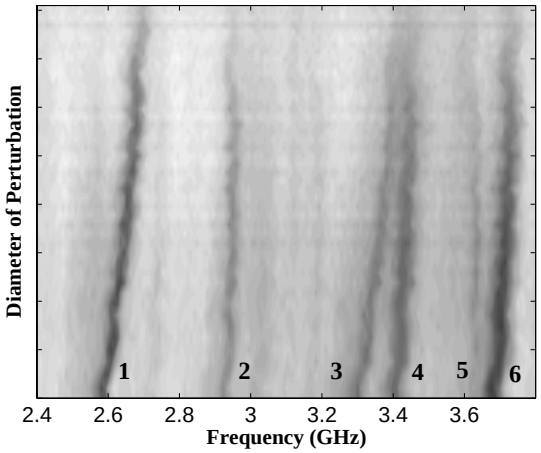

Fig. 7. Change in circular symmetric WGM frequencies through squeezing. Modes 1 and 3 correspond to radial index of 1 with even $(\ell - m)$ index. Modes 4 and 6 have the same $(\ell - m)$ index, but larger radial index than modes 1 and 3. Modes 2 and 5 have tuning rate of zero, corresponding to an odd $(\ell - m)$ index. The y-axis ranges from zero to 250 nm.

When the perturbation is applied along the semiminor axis, all visible modes shift at some nonzero, discreetly spaced tuning rate. In Table 1, the tuning rate of each mode is a = 706 kHz/nm plus some factor of b = 49 kHz/nm.

3.4. Broken Spatial Degeneracy

The final observation we report in this article is of broken degeneracy of the modal spatial profiles. We label different modes that shift at the same rate under the same perturbation members of the same mode family. The different mode families shift at different tuning rates while subject to the same local perturbation. The field distribution of the mode families must have different overlaps with the circular deformation caused by squeezing the resonator along the equator. The tuning rate of the various mode families is strongly dependant on the location of the perturbation. Based on the data presented in (Table 1), as the optical beam circulates around the elliptical resonator its angular field distribution changes along with the change in boundary conditions.

It was found that two mode families shift in frequency at the same rate in the limit of small perturbation along the semimajor axis of the resonator. This observation implies that these two mode families are spatially degenerate in the neighborhood of the perturbation. As the magnitude of the perturbation is increased, the tuning rates of the two mode families begin to diverge (Fig. **??**.) After the magnitude of perturbation is increased further, the two mode families again shift at the same rate.

Both families exhibit the same tuning slope (706 kHz/nm) with different y-intercepts. Beyond the range shown in (Fig. **??**), the proportionality between applied strain and bias voltage is no longer linear.

4. Conclusion

The asymmetric morphology of the high Q WGM resonators allows discreet mechanical tuning of the individual resonant frequencies. All modes shift uniformly under electrical perturbation. Microwave modulation of the elliptical WGMs with low efficiency was also observed. When

#89275 - $15.00 USD Received 1 Nov 2007; revised 4 Jan 2008; accepted 4 Jan 2008; published 29 Jan 2008

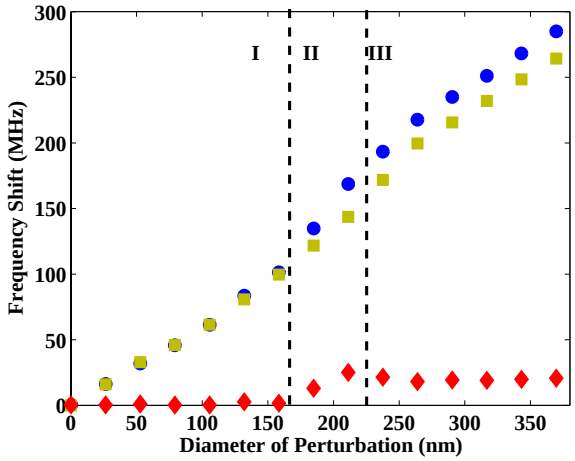

Fig. 8. The frequency shift of two mode families as a function of applied strain. Mode family 1 (blue circles) and 2 (yellow squares) tune at the same rate in region I of Fig. 2. In region II, the tuning rates diverge. The same tuning rate, equal to the rate in region I, is recovered. Red diamonds are residuals of the two tuning rates. The size of the deformation was calculated from measurements of the far field diffraction pattern of the prism-resonator interface.

perturbation is applied locally, there is equivalence in the response of particular resonator mode frequencies to applied perturbation only in certain domains. This suggests symmetry breaking of the mode eigenfunctions.

In the experiments described in this paper, the mechanism behind the reconfigurable spectra is mechanical in nature. This phenomenon can be combined with previously reported high-Q resonances of elliptical WGMs [17] to produce a narrowband optical resonance that does not shift under mechanical oscillation. In addition to the applications outlined in the introduction, this robustness may be attractive for laser frequency stabilization.

Thermal loading leading to low frequency mechanical oscillation in WGM resonators has been reported [23]. Reconfigurable WGM spectra will allow tuning of the mode frequencies to a separation matching the mechanical oscillation frequency, which could in turn enhance the process.

Acknowledgements

The research described in this publication was carried out at the Jet Propulsion Laboratory, California Institute of Technology, under a contract with the National Aeronautics and Space Administration, and with support from DARPA.

#89275 - $15.00 USD Received 1 Nov 2007; revised 4 Jan 2008; accepted 4 Jan 2008; published 29 Jan 2008